Study on the Impact of Multilayer PCB Design with EBG Structure on Noise Suppression and Signal Integrity

Jian-fang Wang.1,*, Chu-Yu Chen.2,*

[1,2.]Department of Electrical Engineering, National University of Tainan, Tainan, 70005, Taiwan

[1*]E-mail : fang10509102@gmail.com
[2*]E-mail : cychen57@mail.nutn.edu.tw

Abstract

This paper investigates the electromagnetic bandgap (EBG) structures in multilayer printed circuit board (PCB). The suppression of simultaneous switching noise (SSN) and the maintenance of signal integrity (SI) are further addressed. A novel EBG design incorporating complementary periodic slot line and via arranged periodically is developed to achieve wideband and high-efficiency common-mode noise suppression. The EBG structure with the noise suppression bandwidth from 0.14 GHz to 50 GHz is proposed and simulated. Furthermore, this design not only effectively attenuates high-frequency noise such as SSN but also provides stable common-mode noise suppression across a wide frequency spectrum. Importantly, the structure suppresses common-mode signals without adversely affecting the transmission of differential-mode signals, thus preserving overall signal integrity. Consequently, this research successfully efficiently filters SSN and other high-frequency noise sources, maintaining signal clarity and accuracy across a broad frequency range.

Keywords: electromagnetic bandgap, simultaneous switching noise, signal integrity, common-mode noise

----
Corresponding author:
fang10509102@gmail.com
cychen57@mail.nutn.edu.tw
DOI:10.53106/222344892026041601003

基於 EBG 結構的四層板設計對雜訊抑制與信號完整性的影響研究

王建方, 陳居毓

國立臺南大學電機工程學系碩士班

摘要

本研究探討了電磁帶隙（EBG）結構在多層印刷電路板（PCB）中的應用，特別是在抑制同步開關雜訊（SSN）和信號完整性（SI）的維護進行探討。研究提出一種創新的EBG設計架構，結合週期性槽線與貫孔(via)週期性的方式排列，達到寬頻且高效率的雜訊抑制效果。本研究設計EBG結構可有效地將抑制頻帶拓展至0.14GHz至50GHz之廣泛範圍。另外此設計不僅能夠有效衰減SSN等高頻雜訊，還能在寬頻範圍內穩定地提供共模信號的抑制。在不影響差分模式信號傳輸的情況下，能夠有效地抑制共模信號，保持信號完整性。因為EBG結構主要影響的是共模信號，而差分信號則能夠在此結構中正常傳播，保持其質量。本研究成功實現了對SSN有效濾除，並且能在廣泛的頻率範圍內保持信號的清晰度與準確性。

關鍵字: 電磁帶隙、開關雜訊、訊號完整性、共模雜訊

1 Introduction

With the advancement in high-speed and miniaturized electronic products, characterized by continuously decreasing clock cycles, increasing data transmission rates, and shrinking electronic components and circuit layouts, simultaneous switching noise and electromagnetic interference (EMI) issues in printed circuit board have become increasingly severe. These issues significantly challenge maintaining signal integrity and power integrity. SSN primarily arises from transient currents generated by multiple electronic components and integrated circuit (IC) switching simultaneously. These currents, interacting with parasitic inductance and capacitance in PCB, cause voltage fluctuations between power and ground planes, adversely affecting overall system power stability and signal quality, and potentially leading to system errors or performance degradation. Electromagnetic bandgap structures, known for their effective noise suppression capabilities within specific frequency ranges, have emerged as vital solutions in PCB design. The periodic arrangement of EBG structures forms broadband resonant structures capable of generating adjustable bandgaps in designated frequency ranges, providing high-impedance planes to effectively suppress noise propagation and achieve extensive noise suppression from low to high frequencies, thereby mitigating SSN interference [1][2][3].

References [4][5] utilized planar electromagnetic bandgap structures, leveraging inductive effects produced by Meander-L Bridges and capacitive effects between unit cell gaps to form parallel resonant circuits. The equivalent circuits illustrate that these periodic structures serve as multi-stage filters, effectively suppressing noise over a broad frequency spectrum. Nevertheless, planar EBG configurations can negatively impact signal integrity, primarily due to elongated return paths, increasing the risk of signal quality deterioration [6].

The concept presented in reference [7] proposes an EBG structure combined with power-and-ground via pairs. It is designed specifically for effective SSN suppression while preserving SI and PI. This structure involves selective etching in noise-generating and sensitive circuit areas, combined with multilayer interconnections through via, thereby circumventing potential adverse effects on signal integrity associated with conventional bridging approaches.

Common SSN mitigation strategies currently in use include decoupling capacitors, precise transmission line techniques, traditional EBG structures, magnetic materials, high-impedance surfaces (HIS), embedded capacitance layers, and ground shielding. Each method has distinct limitations. Decoupling capacitors exhibit reduced effectiveness at higher frequencies due to parasitic inductance. Transmission line techniques require precise impedance control [8], making their widespread application challenging in power distribution networks. Poorly designed traditional EBG structures may increase return path impedance, adversely impacting signal integrity. Additionally, magnetic materials, HIS, embedded capacitance layers, and ground shielding encounter challenges such as high implementation costs, complex fabrication processes, or spatial limitations in high-frequency and high-density PCB environments [9].

This paper proposes an innovative multilayer EBG structure design. By integrating periodic slot line and arrays of via, this design achieves broadband noise suppression. The proposed structure effectively reduces noise within the frequency range of 0.14-50 GHz and effectively mitigates SSN. Simulation validations confirm that this structure significantly suppresses common-mode noise while minimally impacting differential signals. Furthermore, it can effectively reduce the common-mode voltage of differential pairs, preserving signal transmission integrity.

2 Design Methodology

(A) Electromagnetic Bandgap Structures

Electromagnetic Bandgap structures utilize periodic arrangements of conductive and dielectric materials to create specific frequency bandgaps through Bragg Reflection and effectively block electromagnetic wave propagation within these bands. The condition for Bragg Reflection is given by [10]:

$$n\lambda = 2d\sin\theta \qquad (1)$$

Where n represents the order of reflection, λ is the wavelength of the electromagnetic wave, d is the periodic spacing of the structure, and θ is the angle of incidence. When this condition is met, reflected waves from the periodic interfaces constructively interfere, generating distinct electromagnetic bandgaps. The design of EBG structures is influenced by wave number, dispersion, phase velocity, and group velocity, each of which will be discussed in the subsequent sections.

In the design of Electromagnetic Bandgap structure, understanding wave propagation characteristics and dispersion relationships is essential. The wave number k is defined as the number of oscillations per unit length and is related to the wavelength λ and angular frequency ω by：

$$k = \frac{2\pi}{\lambda} = \frac{\omega}{v} \qquad (2)$$

The magnitude of the wave number is strongly related to the physical dimensions of the structure. In EBG structures in particular, lower wave numbers correspond to lower-frequency signals, which require larger unit cell dimensions to achieve effective suppression—thus determining the location and bandwidth of the bandgap.

Dispersion describes the nonlinear relationship between frequency and wave number, commonly expressed as (3)。In dispersive media, waves of different frequencies propagate at different speeds, resulting in signal distortion or pulse broadening. This dispersion relationship is especially critical in EBG structures, as it directly influences the formation of bandgaps and the wave propagation behavior.

$$\omega = f(k) \qquad (3)$$

To characterize wave velocities, two commonly used parameters are the phase velocity v_p and the group velocity v_g：

$$v_p = \frac{\omega}{\beta} \qquad (4)$$

$$v_g = \frac{d\omega}{d\beta} \qquad (5)$$

Phase velocity represents the speed of a constant-phase point on a single-frequency wave, while group velocity corresponds to the speed at which energy or signal envelopes propagate. Group velocity is particularly significant in EBG design since it tends to drop sharply near the bandgap edges and may even approach zero, indicating that wave propagation becomes ineffective within the stopband.

Further analysis of the dispersion relationship and bandgap formation can be expressed through the following dispersion equation：

$$\beta = \sqrt{k^2 - {k_c}^2} \qquad (6)$$

Here, k_c denotes the cutoff wave number. When $k < k_c$, the propagation constant β becomes imaginary, indicating that the wave decays exponentially and cannot propagate—thus forming a stopband or bandgap region. This mechanism forms the physical basis by which EBG structures suppress specific frequency components of electromagnetic waves. By appropriately designing the periodic geometry, one can prevent the establishment of stable propagation modes within certain frequency ranges, thus creating an effective bandgap. This contributes directly to noise suppression and electromagnetic interference control. The analysis of such wave behavior and dispersion is fundamental to the theoretical framework that guides the geometric parameter design of EBG structures.

(B) Analysis of Periodic Structures

According to reference [10], periodic structures can be implemented using microstrip lines or waveguides. When analyzing the propagation properties of periodic structures, the cascaded two-port networks can be represented by the ABCD matrix as follows:

$$\begin{bmatrix} Vn \\ In \end{bmatrix} = \begin{bmatrix} \mathrm{A} & \mathrm{B} \\ \mathrm{C} & \mathrm{D} \end{bmatrix} \begin{bmatrix} \mathrm{V}_{n+1} \\ I_{n+1} \end{bmatrix} \qquad (7)$$

Here, parameters A, B, C, D represent the transmission matrix elements of the two-port network. When two transmission line segments with length d/2 are separated by the shunt susceptance, the ABCD matrix can be expressed as:

$$\begin{bmatrix} A & B \\ C & D \end{bmatrix} = \begin{bmatrix} cos\frac{\theta}{2} & jsin\frac{\theta}{2} \\ jsin\frac{\theta}{2} & cos\frac{\theta}{2} \end{bmatrix} \begin{bmatrix} 1 & 0 \\ jb & 1 \end{bmatrix} \begin{bmatrix} cos\frac{\theta}{2} & jsin\frac{\theta}{2} \\ jsin\frac{\theta}{2} & cos\frac{\theta}{2} \end{bmatrix}$$

$$= \begin{bmatrix} (cos\theta - \frac{b}{2}sin\theta) & j(sin\theta + \frac{b}{2}cos\theta - \frac{b}{2}) \\ j(sin\theta + \frac{b}{2}cos\theta + \frac{b}{2}) & (cos\theta - \frac{b}{2}sin\theta) \end{bmatrix} \qquad (8)$$

Where θ =kd，k denotes the propagation constant of the unloaded transmission line. For an infinitely periodic structure, the voltage and current relationship between adjacent unit cell differs by a propagation factor $e^{-\gamma d}$. For a nontrivial solution, the determinant of the corresponding matrix must be zero, leading to the dispersion relation:

$$\cosh(\gamma \mathrm{d}) = \frac{A+D}{2} = \left(cos - \frac{b}{2}sin\theta\right) \qquad (9)$$

Letting $\gamma = \alpha + j\beta$，the complex propagation constant γ must satisfy the following conditions based on the characteristics of the hyperbolic cosine function:

$$\cosh(\gamma \mathrm{d}) = \cosh(\alpha \mathrm{d})\cos(\beta \mathrm{d}) + \mathrm{j}\sinh(\alpha \mathrm{d})\sin(\beta \mathrm{d}) = \cos\theta - \frac{b}{2}sin\theta \qquad (10)$$

Case 1 (bandpass): $\alpha = 0$，$\beta \neq 0$

In a periodic structure, this condition corresponds to electromagnetic waves that can propagate without attenuation, defining the passband of the structure. Equation (5) can thus be simplified accordingly:

$$\cos(\beta \mathrm{d}) = \cos\theta - \frac{b}{2}sin\theta \qquad (11)$$

Case 2 (band-stop): $\alpha \neq 0$，$\beta = 0, \pi$

In a periodic structure, this case corresponds to non-propagating electromagnetic waves, where the wave attenuates along the transmission line. This region is defined as the stopband of the structure. Since the structure is lossless, the incident wave energy is not dissipated but instead reflected. Equation (12) an thus be simplified in this scenario as well.

$$cos\,h(\alpha d) = \left|cos\theta - \frac{b}{2}sin\theta\right| \geq 1 \qquad (12)$$

Such waves are referred to as Bloch waves, named after their propagation characteristics, which resemble those of elastic waves traveling through periodic crystal lattices.

3 Multilayer Electromagnetic Bandgap Structure Design and Simulations

A four-layer staggered via-based EBG structure implemented on FR4 substrate is developed to ensure cost-effectiveness and compatibility. The multilayer configuration minimizes interlayer spacing to enhance parasitic capacitance and inter-plane coupling. Periodic slot structures are incorporated to excite multiple resonance modes [12], enabling broadband noise suppression.

The initial design parameters of the proposed electromagnetic bandgap unit cell are summarized in Table 1, and the corresponding top and side views are illustrated in Figure 1. Each unit cell measures 10 mm × 10 mm and incorporates two via: one via connects layer 1 and layer 3, while the other connects layer 2 and layer 4. The copper foil thickness follows the standard 1 oz specification, and the overall PCB thickness is preliminarily defined based on the parameters referenced in [9]. The initial simulated S-parameter results of this configuration are presented in Figure 2. As observed from the S-parameters in Figure 2, the initial structure with the −40 dB suppression threshold is limited to the small portion of the frequency spectrum.

To enhance the bandwidth performance, the unit cell configuration was further expanded into a 5×5 array. The sensitivity for different interlayer spacings is simulated and the periodic slot structures are incorporated to excite multimode resonances. It is expected that the larger parallel-plate capacitance, the wider the suppression bandwidth. and incorporating periodic slot structures to excite multimode resonances.

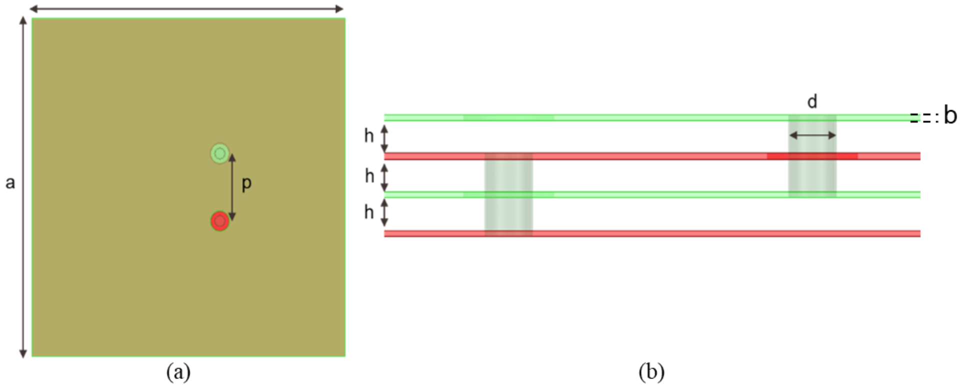

Figure 1:(a) Top View of the Unit Cell; (b) Side View

Table 1:Parameters of the Electromagnetic Bandgap Structure

parameters	length(mm)	parameters	length(mm)
a	10	d	0.3
p	2	b	0.035
h	0.1	ε_r	4.4

(d: via diameter, b: copper thickness)

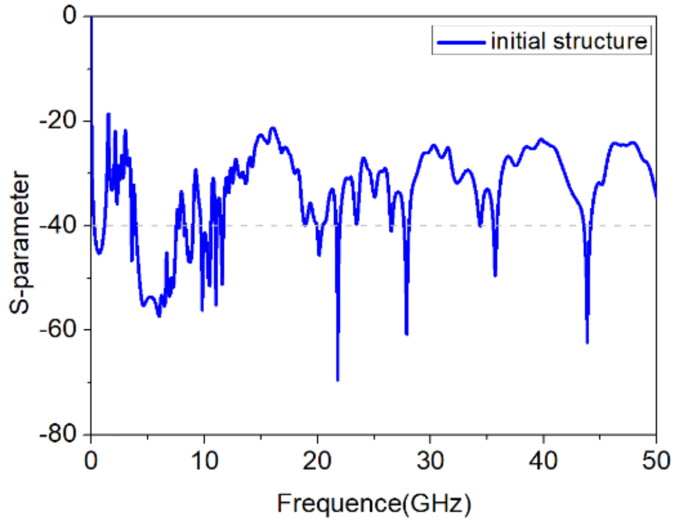

Figure 2:Initial S-Parameters of the Electromagnetic Bandgap Structure

Multilayer architectures are effective in providing the capacitive characteristics of EBG structures [9]. As described by the parallel-plate capacitance equation (13), the capacitance increases as the separation distance d between layers decreases. This increasing of parasitic capacitance improves the structure’s ability to suppress noise. Although a smaller interlayer distance also results in a slight reduction in the parasitic inductance associated with via, its effect on overall performance is negligible.

The S-parameter results shown in Figure 3 further validate this observation. As the interlayer spacing h decreases from 0.10 mm to 0.04 mm, the suppression depth and range are significantly improved, especially in the low-frequency region. In Figure 3, the importance of interlayer spacing in broadband noise suppression is confirmed and the enhanced performance in the low-frequency range below 3 GHz is highlighted. However, due to practical fabrication limitations, the layer spacing cannot be indefinitely reduced.

$$C = \frac{\epsilon A}{d} \tag{13}$$

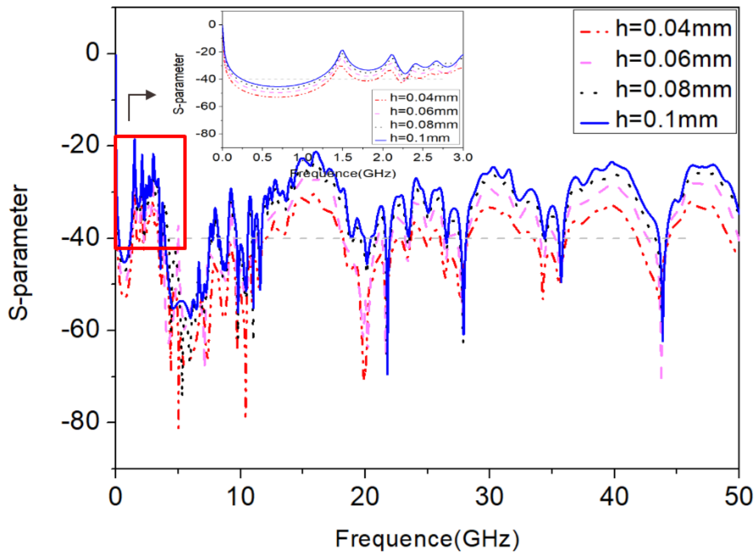

Figure 3:S-Parameter Analysis of EBG Structure with Varying Interlayer Spacing

To address this constraint while maintaining suppression effectiveness, periodic slot structures are subsequently introduced to excite multimode resonances and widen the suppression bandwidth. Two complementary enhancement techniques are adopted for this purpose.

(A) Technique1:Periodic Slot Arrays and Bridge-Integrated EBG Design

The structure and layout of the slot-line EBG unit cell are illustrated in Figure 4, where (a) shows the top view and (b) presents the embedded configuration. Detailed dimensional parameters are listed in Table 2. The periodic slot arrays and bridge structures are implemented on layers 2 and 4 to introduce additional resonant modes. This hybrid design effectively broadens the stopband and enhances high-frequency noise suppression. Simulation results indicate that the optimized slot and bridge configuration significantly improves suppression depth and bandwidth. The unique resonant modes generated by the periodic slot-line arrangement can provide the high-impedance surface (HIS) characteristics. This effectively suppresses simultaneous switching noise and makes the design well-suited for high-speed electronic applications. However, to maintain signal integrity, it is essential to reduce slot spacing and ensure proper return path configurations when integrating bridge structures.

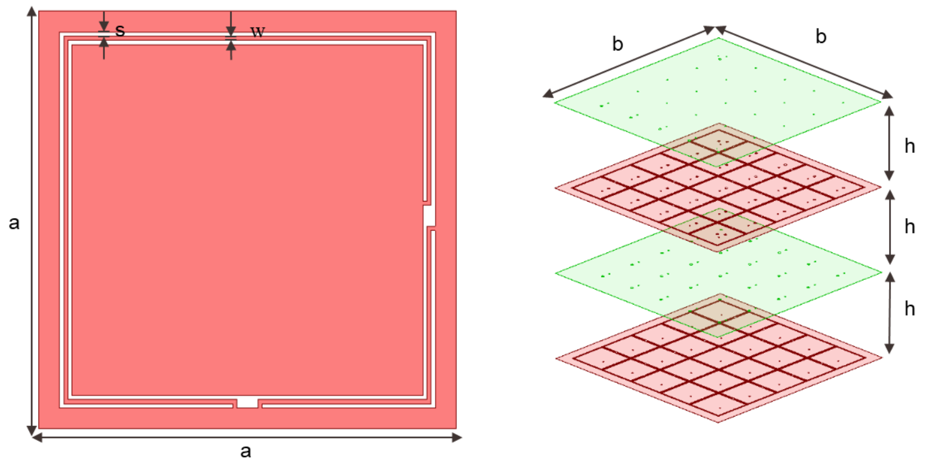

(a) (b)

Figure 4:(a) Top View of the Unit Cell with Slot-Line; (b) Embedded Slot-Line Top View

Table 2:Parameters of the Slot-Line EBG Structure

參數	長度(mm)	參數	長度(mm)
a	10	b	50
s	0.1	h	0.04
w	0.1	ε_r	4.4

(B) Technique2:Current-Distribution-Based Via Placement Optimization

Although the implementation of slot and bridge structures significantly improved the overall suppression performance, certain frequency ranges still failed to meet the −40 dB criterion. To further enhance suppression effectiveness in these regions, a detailed current distribution analysis was conducted at 16 GHz. As illustrated in Figure 5(a), areas exhibiting concentrated current density were identified as critical pathways for high-frequency noise propagation.

Upon closer examination, it is found that the current density was predominantly concentrated near the signal source. This observation indicates that the source region serves as a major coupling point for high-frequency noise transmission. In response to this finding, additional via were strategically placed around the high-current-density areas near the source, aiming to strengthen suppression at the corresponding frequencies. Under high-frequency excitation, via inherently possess parasitic inductance; when paired with the surrounding conductive layers, they form localized capacitive structures that behave similarly to resonant cavities. This equivalent circuit behavior gives rise to resonance at specific frequencies, thereby generating a high-impedance surface that effectively reflects and suppresses electromagnetic wave propagation. As a result, enhanced broadband noise suppression was achieved, further improving the overall performance of the proposed EBG structure.

Figure 5(b) illustrates the optimized via placement, which effectively addresses high current zones. This enhancement, when combined with the slot and bridge integration, yields a robust and broadband suppression mechanism.

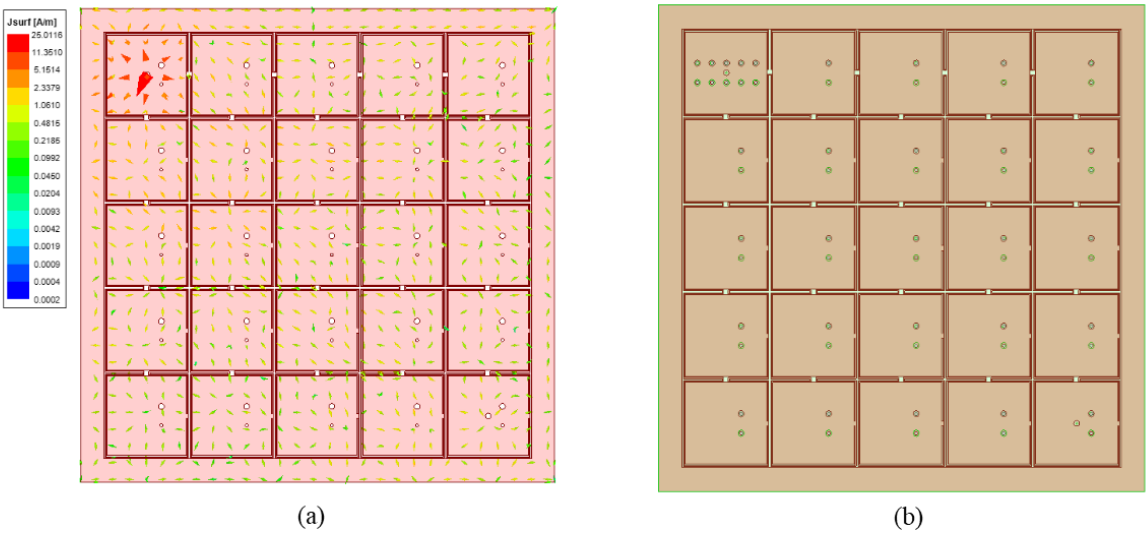

Figure 5:(a) Current Distribution at 16 GHz; (b) Top View of Via Placement Optimization

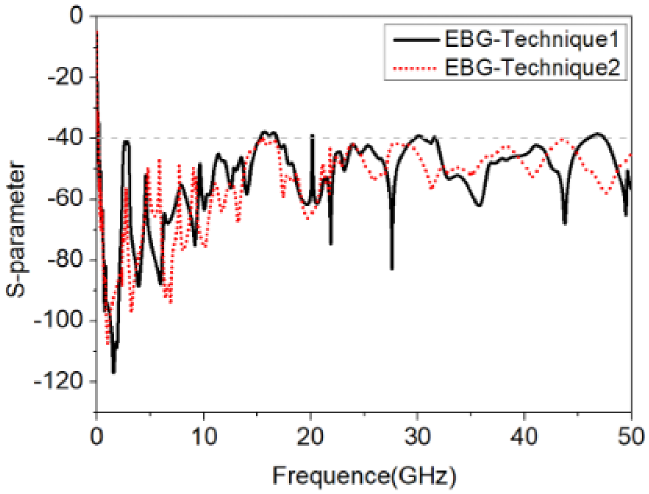

Figure 6:S-Parameters Illustrating Broadband Noise Suppression of the Electromagnetic Bandgap Structure

Simulation results confirm that the introduction of via in regions of elevated current density further enhances the filtering performance of the EBG structure. Frequency bands that previously only marginally exceeded the -40 dB threshold were successfully suppressed below the target level after optimization. The added via not only reinforced local noise isolation but also extended the overall bandgap range of the structure. As shown in Fig. 6, the suppression bandwidth was expanded 0.14–50 GHz, demonstrating that the proposed structure offers robust and broadband suppression of simultaneous switching noise.

4 Signal Integrity Analysis and Simulation results

As previously discussed, although Electromagnetic Bandgap structures exhibit excellent noise suppression capabilities, they typically involve patterning the power or ground planes. This patterning disrupts the continuity of the reference plane, extending signal return paths and consequently affecting signal integrity[13][14]. However, with appropriate design considerations, EBG structures not only effectively mitigate simultaneous switching noise but also substantially suppress common-mode noise generated by mismatch differential pair [15]. The impact of the EBG reference plane on differential signal integrity and common-mode noise suppression in microstrip line structures is further evaluated.

(A) Common mode and differential mode Analysis

Both differential-mode and common-mode transmission characteristics of microstrip lines referenced to a solid ground plane and an EBG plan are investigated. The S-parameters Sdd21 and Scc21 are defined in Equations (15) and (16). Simulation results show that Sdd21 responses of both reference structures overlap closely, indicating minimal impact on differential-mode signal integrity when using an EBG reference plane. However, significant suppression is observed in Scc21 when the EBG structure is employed, demonstrating effective attenuation of common-mode noise propagation. This analysis highlights the advantage of the EBG structure, which suppresses common-mode noise without compromising differential-mode signal integrity.

Further analysis was conducted in the time domain using circuit simulation software with differential input voltages set to ±500 mV. As shown in Figure 7 Differential-mode voltage is defined as the difference between the two output voltages, while common-mode voltage is defined as half the sum of the two output voltages. As shown in Figure 8 Time-domain waveforms show that the differential-mode signals remain largely unaffected when the EBG reference plane is used, thus maintaining excellent signal integrity. In contrast, the common-mode voltage is significantly suppressed, confirming the effectiveness of the EBG structure in mitigating common-mode noise. These results indicate that the EBG reference plane provides effective noise filtering in both frequency and time domains, making it highly suitable for common-mode noise control in high-speed differential signaling systems.

$$S_{dd21} = 20\log_{10}\frac{V_{diff\_out}}{V_{diff\_in}} \quad (15)$$

$$S_{cc21} = 20\log_{10}\frac{V_{commom_{out}}}{V_{common_{in}}} \quad (16)$$

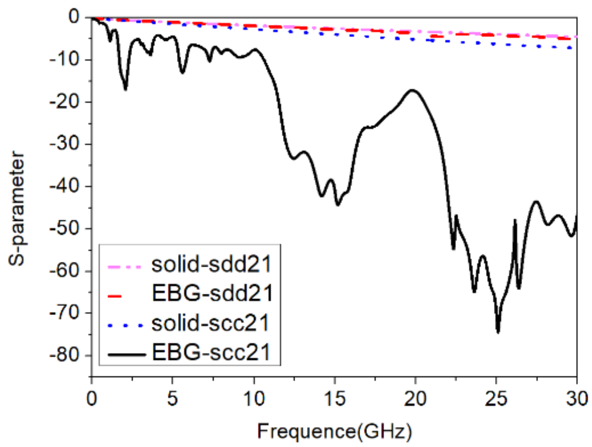

Figure 7:S-Parameters of Microstrip Line with Solid Reference Plane and EBG Reference Plane

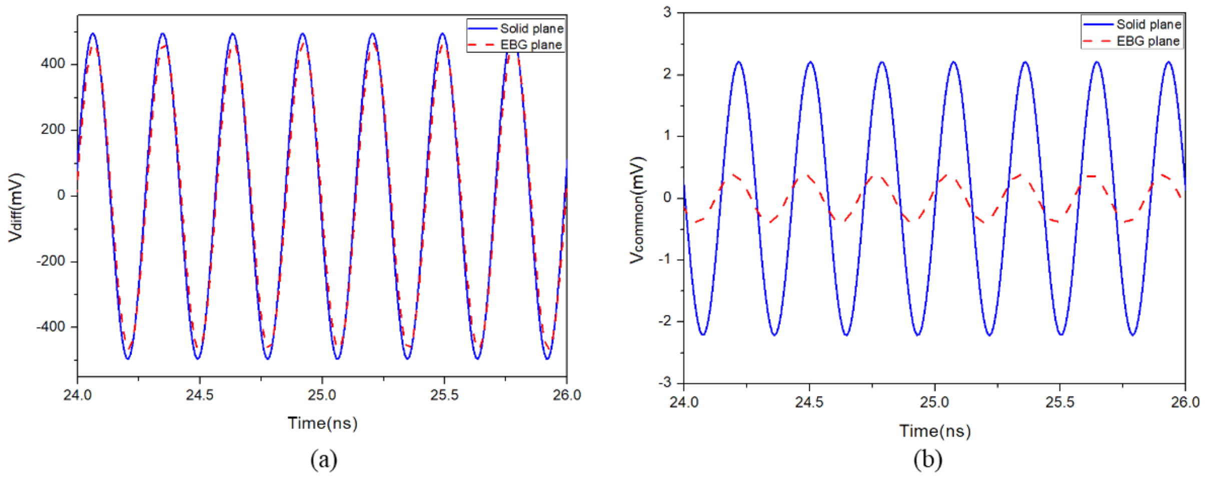

Figure 8:Voltage Analysis of Microstrip Line with Solid and EBG Reference Planes

(a) Differential-Mode Voltage (b) Common-Mode Voltage

(B) Crosstalk Analysis

Crosstalk arises due to electromagnetic coupling between two adjacent conductors. Specifically, a voltage change on one conductor creates a changing electric field, which, through parasitic capacitance (mutual capacitance), induces a current variation in the neighboring conductor. Similarly, a current change in one conductor produces a changing magnetic field, which, through parasitic inductance (mutual inductance), induces voltage fluctuations in the adjacent conductor.

In this study, a differential signaling environment was simulated to evaluate the impact of crosstalk on an adjacent single-ended line, using both a conventional solid ground plane and the proposed EBG reference plane. The circuit configuration for the crosstalk simulation is illustrated in Figure 9, where differential signals are driven on line, and the resulting noise is observed on a neighboring victim line at both the near-end and far-end locations.

The input differential voltage was set to ±500 mV. The resulting near-end and far-end crosstalk voltage waveforms are presented in Figure 10. As shown in Figure 10(a) and Figure 10(b), the EBG reference plane performs comparably to the solid ground plane in terms of suppressing both near-end crosstalk (NEXT) and far-end crosstalk (FEXT). This confirms that the EBG structure, while effectively suppressing common-mode noise and enabling broadband filtering, does not compromise signal isolation or electromagnetic compatibility (EMC).

These results validate that the proposed EBG reference plane offers superior noise mitigation while maintaining acceptable crosstalk levels, thereby preserving high signal integrity and ensuring reliable operation in dense, high-speed PCB environments.

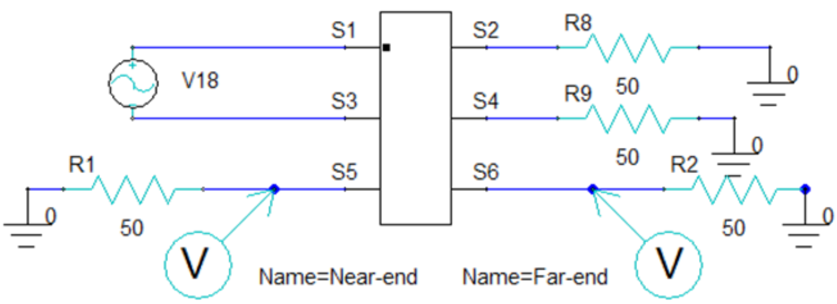

Figure 9:crosstalk circus

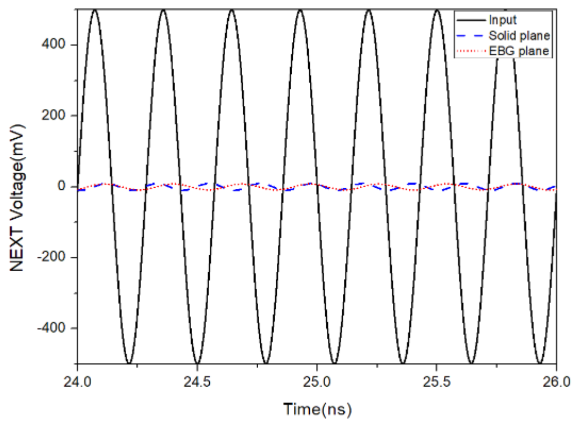

(a)

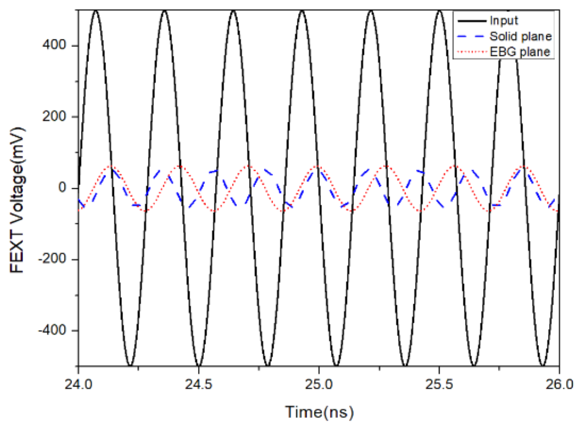

(b)

Figure 10:Crosstalk Comparison Between Solid and EBG Reference Planes (a) Near-End Crosstalk; (b) Far-End Crosstalk

(C) Eye Diagram Analysis

The eye diagram is a widely adopted time-domain analytical tool used to evaluate the integrity of high-speed digital signals by visually representing variations in timing and voltage levels. In such diagrams, the eye width indicates the duration of signal stability within each bit period, serving as a key metric for timing jitter. The eye height, on the other hand, represents the voltage margin relative to the receiver's threshold levels (VIH and VIL), thus aiding in determining safe and reliable sampling points. Greater eye width and height typically suggest lower jitter and minimal inter-symbol interference (ISI), ensuring improved signal quality and system robustness [17].

As shown in Figure 11, the eye diagrams obtained using both a solid reference plane and the proposed EBG reference plane are analyzed. Figure 11(a) illustrates the eye diagram with a solid ground reference, while Figure 11(b) presents the result with the EBG reference plane. It is observed that the EBG structure have a slight reduction in eye height—from 2.03 to 1.96421 V—and eye width—from 284.84 to 282.99 ps compared to the case of the solid ground reference. These reductions of approximately 3% in eye height and 0.6% in eye width remain well within acceptable margins and the signal integrity is not significantly compromised. The clarity of the eye opening remains intact and jitter remains minimal (0.08 UI for solid plane vs. 0.0896UI for EBG). This confirms that the proposed EBG design effectively mitigates simultaneous switching noise while maintaining high signal fidelity, making it suitable for use in high-speed differential signal environments.

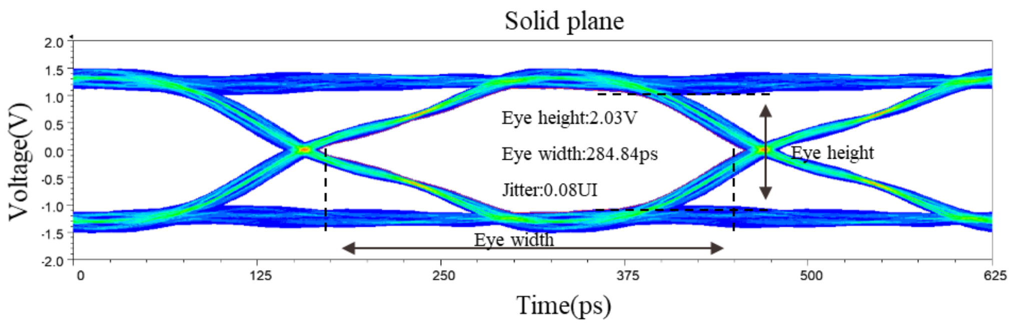

(a)

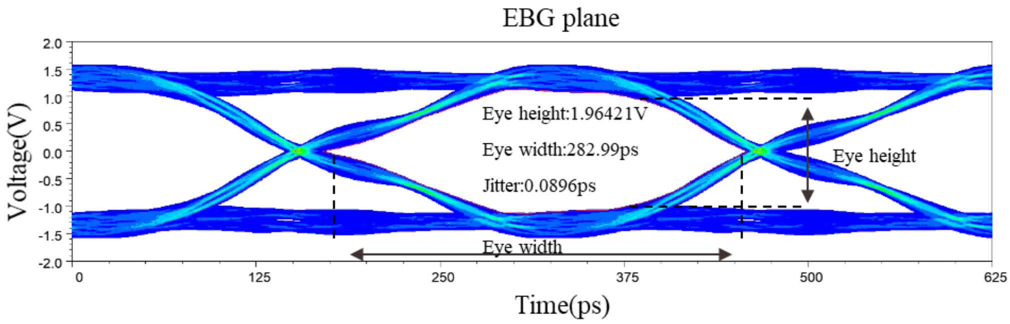

(b)

Figure 11: Eye Diagram (a) With Solid Reference Plane; (b) With EBG Reference Plane

5 Conclusion

This paper presents a broadband simultaneous switching noise suppression structure based on a multilayer staggered electromagnetic bandgap structure. By utilizing a staggered structure arrangement, enhanced parasitic capacitance is generated, effectively lowering the cutoff frequency and improving low-frequency noise suppression capability. Furthermore, precise adjustments of layer spacing integrated with periodic slot-line design enable excitation of multiple electromagnetic resonant modes and further extend the noise suppression bandwidth.

Under the criterion of the effective SSN suppression, simulation results demonstrate that the proposed structure achieves broad-spectrum SSN filtering from approximately 0.14 GHz to 50 GHz. Eye diagram evaluations further confirm minimal impact on differential signal quality, maintaining excellent overall signal integrity. Consequently, the proposed design fulfills both noise suppression and electromagnetic compatibility requirements for high-speed digital circuits, while simultaneously ensuring superior high-speed signal transmission quality.

Reference

[1] M. R. Bansode and S. S. Rathod, "Enhanced Signal and Power Integrity using Novel Planar EBG design," 2023 Joint Asia-Pacific International Symposium on Electromagnetic Compatibility and International Conference on ElectroMagnetic Interference & Compatibility (APEMC/INCEMIC), Bengaluru, India, 2023

[2] S. -G. Kim, H. Kim, H. -d. Kang and J. -G. Yook, "Signal Integrity Enhanced EBG Structure With a Ground Reinforced Trace," in IEEE Transactions on Electronics Packaging Manufacturing, vol. 33, no. 4, pp. 284-288, Oct. 2010

[3] L. -F. Shi, G. Zhang, M. -M. Jin, S. Chen and X. -J. Hu, "Novel Subregional Embedded Electromagnetic Bandgap Structure for SSN Suppression," in IEEE Transactions on Components, Packaging and Manufacturing Technology, vol. 6, no. 4, pp. 613-621, April 2016

[4] L. -F. Shi, Z. -M. Sun, G. -X. Liu and S. Chen, "Hybrid-Embedded EBG Structure for Ultrawideband Suppression of SSN," in IEEE Transactions on Electromagnetic Compatibility, vol. 60, no. 3, pp. 747-753, June 2018

[5] L. -F. Shi, K. -J. Li, H. -Q. Hu and S. Chen, "Novel L-EBG Embedded Structure for the Suppression of SSN," in IEEE Transactions on Electromagnetic Compatibility, vol. 58, no. 1, pp. 241-248, Feb. 2016

[6] F. De Paulis, L. Raimondo, B. Archambeault, S. Connor and A. Orlandi, "Compact configuration of a planar EBG based CM filter and crosstalk analysis," 2011 IEEE International Symposium on Electromagnetic Compatibility, Long Beach, CA, USA, 2011,

pp. 704-709, doi: 10.1109/ISEMC.2011

[7] Z. -C. Yang and H. -R. Zhu, "Power Noise Suppression Using Power-and-Ground via Pairs for Signal and Power Integrity," 2023 International Applied Computational Electromagnetics Society Symposium (ACES-China), Hangzhou, China, 2023, pp. 1-3, doi: 10.23919/ACES-China60289.2023

[8] Wen-Hua Tu and Kai Chang, "Compact second harmonic-suppressed bandstop and bandpass filters using open stubs," in IEEE Transactions on Microwave Theory and Techniques, vol. 54, no. 6, pp. 2497-2502, June 2006

[9] C. -D. Wang and T. -L. Wu, "Model and Mechanism of Miniaturized and Stopband-Enhanced Interleaved EBG Structure for Power/Ground Noise Suppression," in IEEE Transactions on Electromagnetic Compatibility, vol. 55, no. 1, pp. 159-167, Feb. 2013

[10] Pozar David m.,and David M Pozar. Microwave Engineer,Wiley 2012

[11] G. Sun et al., "A Novel Broadband EBG Structure For Simultaneous Switching Noise Suppression," 2023 International Applied Computational Electromagnetics Society Symposium (ACES), Monterey/Seaside, CA, USA, 2023

[12] M. Yuan, H. Chen, W. Che and Q. Xue, "A Broadband Hybrid-Embedded EBG Structure for Suppressing Simultaneous Switching Noise," 2024 IEEE International Conference on Computational Electromagnetics (ICCEM), Nanjing, China, 2024

[13] F. De Paulis, A. Orlandi, L. Raimondo and G. Antonini, "Fundamental mechanisms of coupling between planar electromagnetic bandgap structures and interconnects in high-speed digital circuits. Part I - microstrip lines," 2009 International Symposium on Electromagnetic Compatibility - EMC Europe, Athens, Greece, 2009

[14] F. de Paulis, L. Raimondo, D. Di Febo and A. Orlandi, "Routing strategies for improving common mode filter performances in high speed digital differential interconnects," 2011 IEEE 15th Workshop on Signal Propagation on Interconnects (SPI), Naples, Italy, 2011

[15] F. De Paulis, A. Orlandi, L. Raimondo, B. Archambeault and S. Connor, "Common mode filtering performances of planar EBG structures," 2009 IEEE International Symposium on Electromagnetic Compatibility, Austin, TX, USA, 2009

[16] R. Mudavath and B. R. Naik, "Estimation of Far End Crosstalk and Near End Crosstalk Noise with Mutually Coupled RLC Interconnect Models," 2018 International Conference on Communication and Signal Processing (ICCSP), Chennai, India, 2018

[17] Y. Oh, D. Han, B. Go, S. Lee and W. Jeong, "Novel Eye Diagram Estimation Technique to Assess Signal Integrity in High-Speed Memory Test," 2020 IEEE International Test Conference (ITC), Washington, DC, USA, 2020